Turkish Journal of Physics

Volume 41 | Number 6 Article 5

1-1-2017

# Elastic scattering analysis of $^{12}$C+$^{24}$Mg by WKB method

ORHAN BAYRAK

TÜBİTAK

Turkish Journal of Physics

http://journals.tubitak.gov.tr/physics/

Research Article

Turk J Phys
(2017) 41: 520 – 525

doi:10.3906/fiz-1705-13

# Elastic scattering analysis of $^{12}$C+$^{24}$Mg by WKB method

**Orhan BAYRAK***
Department of Physics, Faculty of Science, Akdeniz University, Antalya, Turkey

**Received:** 15.05.2017 • **Accepted/Published Online:** 20.07.2017 • **Final Version:** 18.12.2017

**Abstract:** We present the elastic scattering analysis of the $^{12}$C+$^{24}$Mg system by using the WKB approximation method within the framework of the barrier-internal wave decomposition over a wide range of energy from $E_{lab}$ = 16 MeV to 24.0 MeV. The results obtained are good agreement with the quantum mechanical (QM) calculation and experimental data.

**Key words:** Elastic scattering, $^{12}$C+$^{24}$Mg, barrier-internal waves, WKB method

## 1. Introduction

The elastic scattering data of the $^{12}$C+$^{24}$Mg system are measured by Sciani et al. [1] in laboratory energies from $E_{lab}$ = 16 MeV to 24.0 MeV. Since the measured data are under and above the Coulomb barrier, the elastic scattering cross section patterns have a strongly oscillatory structure at forward, intermediate, and backward angles. These sorts of experimental data are very important in order to understand the features of nuclear potential. In the literature, the $^{12}$C+$^{24}$Mg system is extensively examined by using some theoretical models. Since there is anomalous large angle scattering (ALAS) in the elastic scattering cross section of the $^{12}$C+$^{24}$Mg system, this system cannot be explained by a standard optical model parameter. Sciani et al. use a shallow and energy-dependent potential parameter and investigate the elastic and inelastic scattering data of the $^{12}$C+$^{24}$Mg system by optical and coupled channels methods [1]. Lichtenthäler et al. examine elastic scattering data of this system by parametrized phase shift method [2]. Boztosun et al. propose a new coupling potential, which has attractive and repulsive terms as distinct from the standard model, in order to explain the elastic and inelastic scattering data of the $^{12}$C+$^{24}$Mg system, simultaneously [3–5]. Karakoc et al. investigate the elastic and fusion cross section data of the $^{12}$C+$^{24}$Mg system by the microscopic $\alpha$–$\alpha$ double folding cluster potential [6]. We examine the elastic scattering of this system with a comparative study of the shallow and deep optical potentials [7]. We also modify nuclear potential at the surface region with two small potentials in addition to the nuclear potential. The presence of the two small additional potentials creates a deepening in the surface region of the nuclear potential. We also show that two small additional potentials take into account the coupling effect like that of the coupled channels calculation [8]. In this paper, within the framework of the internal and barrier wave decomposition concept, which is important to understand the oscillatory structure of the scattering cross section, we examine the elastic scattering of the $^{12}$C+$^{24}$Mg system by using the WKB method over a wide range of energy from $E_{lab}$ = 16 MeV to 24.0 MeV. In the next section, we present the nuclear potential and WKB method. In Section 3, we present the results and discussion.

*Correspondence: bayrak@akdeniz.edu.tr

## 2. Model and method

The effective potential, which describes the elastic scattering of the $^{12}$C+$^{24}$Mg system, is given by

$$V_{eff}(r) = V_l(r) + V_N(r) + V_C(r), \tag{1}$$

where $V_l(r)$, $V_N(r)$, and $V_C(r)$ are the centrifugal, nuclear, and Coulomb potentials, respectively. The modified centrifugal potential is [9]

$$V_l(r) = \frac{(l+1/2)^2\hbar^2}{2\mu r^2}, \tag{2}$$

where $l(l+1) \rightarrow (l+1/2)^2$ and $\mu$ is reduced mass of the colliding pair. The nuclear potential has a volume type real and imaginary Woods–Saxon form factor as

$$V_N(r) = V(r) + W(r) = -\frac{V_0}{1+Exp(\frac{r-R_V}{a_V})} - i\frac{W_0}{1+Exp(\frac{r-R_W}{a_W})}, \tag{3}$$

where $V_0, R_V$ , and $a_V$ are depth, radius, and diffuseness parameters of the real nuclear potential. $W_0, R_W$ , and $a_W$ are depth, radius, and diffuseness parameters of the imaginary nuclear potential. Nuclear potential radius can be given by $R_{V,W} = r_{V,W}(A_p^{1/3} + A_t^{1/3})$ . $A_p$ and $A_t$ are the mass number of projectile and target nucleus. Since the Coulomb potential of a charged projectile particle $Z_p e^2$ interacting with a charged target particle $Z_t e^2$ distributed uniformly over a sphere of radius $R_C$ has a discontinuity at $r = R_C$, we use a modified version of the Coulomb potential as [10,11]

$$\begin{aligned} &V_C(r) = \tfrac{Z_p Z_t e^2}{r}\left[1 - \exp\left\{-vr - \tfrac{1}{2}(vr)^2 - 0.35(vr)^3\right\}\right], \\ &vR_C = 3/2, \;\; R_C = 2.3A_t^{1/3}, \end{aligned} \tag{4}$$

where $Z_p$, $Z_t$, and $R_C$ denote atomic numbers of the projectile and target nucleus as well as the Coulomb radius, respectively. The interaction between $^{12}$C and $^{24}$Mg nuclei is represented in Figure 1. The effective potential has a potential pocket at the range of $r_3 < r < r_2$ and is repulsive for out of this range. The potential pocket disappears while the angular momentum increases in Figure 1. The depth and form of the potential pocket are very important in order to explain observables of nuclear reactions. The turning points can be found the roots of equation $E_{cm} = V_{eff}(r)$ for any angular momentum quantum number. In Figure 2 we plot the complex turning points as a function of angular momentum quantum number. The pole points for real $V(r)$ and complex $W(r)$ nuclear potentials can be calculated by using the formula $r_{V,W} = R_{V,W} + (2n+1)i\pi a_{V,W}$ with $n$ integer numbers. The pole points are shown for real and imaginary potentials in Figure 2. More turning and pole points can also be found for increasing nuclear radius and n numbers, but the contribution of these turning and pole points to the elastic scattering cross section is very small.

The scattering matrix element or the S-matrix produced by the scattered waves from the outside and inside of the potential barrier is [10,11]

$$e^{2i\delta} = \eta_B + \eta_I = \frac{e^{2i\delta_1}}{N_1} + \frac{e^{2i\delta_3}}{N_1(N_1 + e^{2iS_{32}})}, \tag{5}$$

where $\eta_B$ and $\eta_I$ are the reflection coefficients representing the scattering waves from barrier and internal

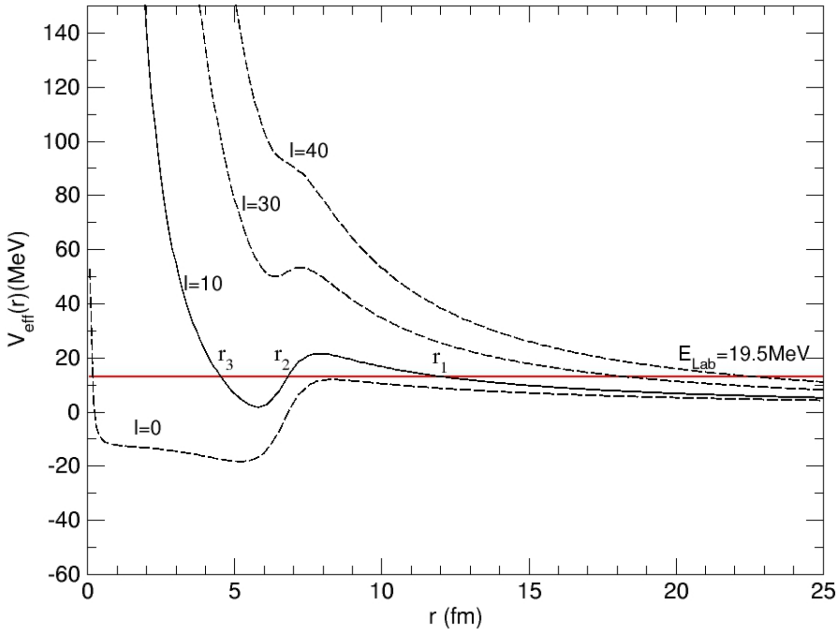


**Figure 1.** The real effective potential for some orbital angular momentum quantum numbers represents interaction between $^{12}$C and $^{24}$Mg nuclei. $r_1$, $r_2$, and $r_3$ denote the turning points. $E_{lab}$ is the projectile energy in the laboratory frame.

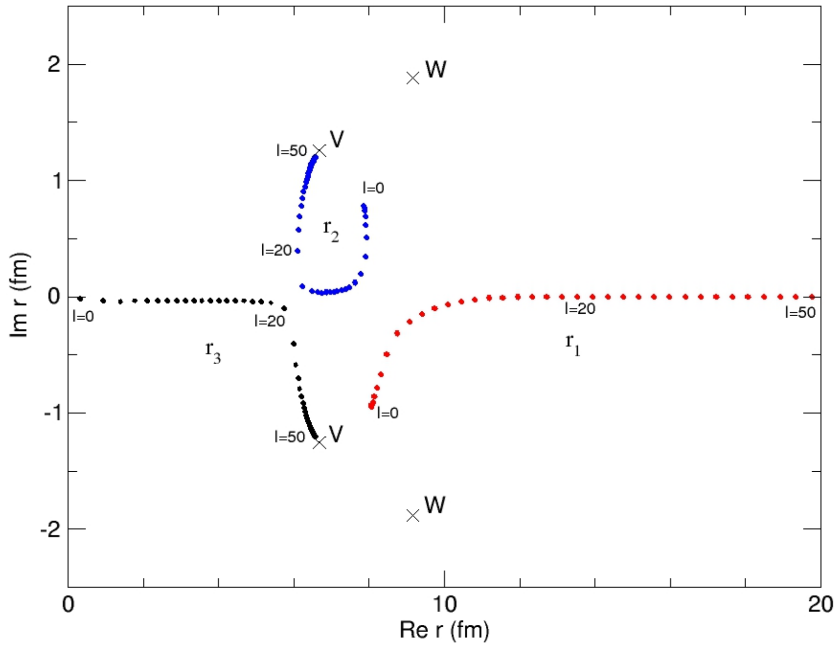


**Figure 2.** The complex turning points of the effective potential as a function of angular momentum quantum numbers in complex plane. × Symbols denote the pole points of complex nuclear potential in Eq. (3).

regions. The phase shift for outermost turning point is defined as [10,11]

$$\delta_1 = S(r_1, R) - S_C(r_c, R) = \sqrt{\frac{2\mu}{\hbar^2}} \left( \int_{r_1}^{R} \sqrt{E_{cm} - V_{eff}(r)} dr - \int_{r_C}^{R} \sqrt{E_{cm} - V_C(r) - V_l(r)} dr \right), \tag{6}$$

where $r_1$, $r_C$, and $R$ are the outermost and Coulomb turning points as well as far enough distance where the Coulomb potential has no effect, respectively. The Coulomb turning point is determined by the root of equation $E_{cm} = V_l(r) - V_C(r)$. $N_1(z)$ coefficient is

$$N_1(z) = \frac{\sqrt{2\pi}}{\Gamma(\frac{1}{2}+z)} \exp(z\ln(\frac{z}{e})), \qquad z = \frac{1}{\pi} S(r_2, r_1), \tag{7}$$

where the action integral for $r_2$ and $r_1$ turning points is

$$S(r_2, r_1) = S_{21} = \int_{r_2}^{r_1} \sqrt{\frac{2\mu}{\hbar^2}\left(E_{cm} - V_{eff}(r)\right)}, \tag{8}$$

The phase shift for the innermost turning point is defined as [10,11]

$$\delta_3 = \sqrt{\frac{2\mu}{\hbar^2}} \left( \int_{r_3}^{R} \sqrt{E_{cm} - V_{eff}(r)} dr - \int_{r_C}^{R} \sqrt{E_{cm} - V_C(r) - V_l(r)} dr \right), \tag{9}$$

The action integral in Eq. (5) $S_{32}$ can be obtained using Eq. (8) for $r_3$ and $r_2$ turning points. The scattering amplitude represented by the scattering waves from the barrier of the effective potential is

$$f_B(\theta) = f_C(\theta) + \frac{1}{2ik} \sum_l (2l+1) P_l(\cos\theta) \exp(2i\sigma_l)(\eta_B - 1), \tag{10}$$

where the reflection coefficient $\eta_B$ can be obtained by using Eq. (5). The Coulomb phase shift for any $l$ states is defined by the recursion relation as

$$\sigma_{l+1} = \sigma_l + \tan^{-1}(\frac{\eta}{l+1}). \tag{11}$$

The Coulomb phase shift is $\sigma_0 = Arg\Gamma(1+i\eta)$ for $l = 0$. Here $\eta$ is the Sommerfeld parameter and is defined by

$$\eta = \frac{Z_p Z_t e^2 \mu}{\hbar^2 k}, \tag{12}$$

where $k^2 = \frac{2\mu E_{cm}}{\hbar^2}$. The Coulomb scattering amplitude in Eq. (10) is given by [12]

$$f_C(\theta) = -\frac{\eta}{2k\sin^2(\frac{\theta}{2})} \exp\left(-i\eta\ln(\sin^2(\frac{\theta}{2})) + 2iArg\Gamma(1+i\eta)\right). \tag{13}$$

The scattering amplitude represented by the scattering waves from inside of the effective potential is

$$f_I(\theta) = \frac{1}{2ik} \sum_l (2l+1) P_l(\cos\theta) \exp(2i\sigma_l)\eta_I, \tag{14}$$

where the reflection coefficient $\eta_I$ can be obtained by using Eq. (5). The total scattering amplitude consists of superposition of the barrier and internal wave scattering amplitudes $f(\theta) \cong f_B(\theta) + f_I(\theta)$ [12]. The total elastic scattering cross section is $\sigma(\theta) = |f(\theta)|^2$.

## 3. Results and discussion

In this paper, we investigate elastic scattering of the $^{12}C+^{24}Mg$ system by using the WKB approximation method. In the calculation we use the effective potential in Eq. (1). The nuclear potential parameters in Eq. (3) are $r_V = 1.29fm$ and $a_V = 0.4\,fm$ for real and $r_W = 1.77fm$ and $a_W = 0.6\,fm$ for imaginary potential. The depth parameters of real and imaginary potential in Eq. (3) change as a function of incident energy of projectile nucleus in the Table.

**Table.** Variation in the depth parameters of real and imaginary potential versus incident energy of projectile nucleus in laboratory frame.

| $E_{lab}$ (MeV) | 16.00 | 17.00 | 19.50 | 20.50 | 23.00 |
|---|---|---|---|---|---|
| $V_0$ (MeV) | 42.10 | 42.82 | 38.00 | 37.75 | 36.20 |
| $W_0$ (MeV) | 0.15 | 0.30 | 0.53 | 0.62 | 0.77 |

We calculate the elastic scattering cross section of the $^{12}C+^{24}Mg$ system over a wide range of energy by using the WKB method taking into account the barrier and internal wave interference effect. The interference between the barrier and internal waves produces an oscillation pattern in elastic scattering cross section in Figure 3. While the incident energy of nucleus increases, the minima and maxima in oscillatory structures of elastic scattering cross section increase at large scattering angles, in particular. This situation shows that incident wave is affected by nuclear potential and internal wave amplitude increases. Therefore, the internal and barrier waves have comparable amplitude and constitute constructive and destructive diffraction patterns in elastic scattering cross section in Figure 3. For the same potential parameters, we also numerically calculate the elastic scattering cross section of the $^{12}C+^{24}Mg$ system by using the quantum mechanical (QM) procedure with FRESCO code (by Thompson, I. J., unpublished) in Figure 3. We show that the theoretical results, WKB

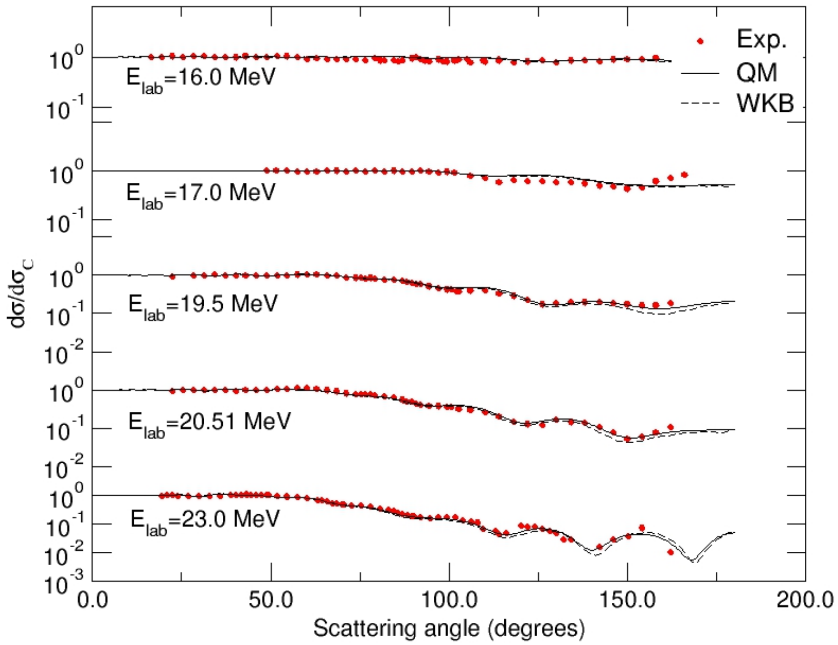


**Figure 3.** The comparative results of elastic scattering cross section data (Exp.) of the $^{12}C+^{24}Mg$ system with quantum mechanical (QM) and WKB methods over a wide range of energy.

and QM, have an excellent agreement with the elastic scattering cross section of experimental data. We also find that the WKB and QM results have good agreement with each other at small angles, in particular.

In conclusion, the WKB method used in this calculation is very useful in order to understand the oscillatory structure in the elastic scattering cross section of the $^{12}C+^{24}Mg$ system and this method could be used in the calculation of other nuclear reaction observables such as inelastic and fusion cross sections.

**Acknowledgment**

This work was supported by the scientific research projects units of Akdeniz University.

## References

[1] Sciani, W.; Lepine-Szily, A.; Lichtenthäler, R.; Fachini, P.; Gomes, L. C.; Lima, G. F.; Obuti, M. M.; Oliveira Jr., J. M.; Villari, A. C. C. *Nucl. Phys. A* **1997**, *620*, 91-113.

[2] Lichtenthäler, R.; Lepine-Szily, A.; Hussein, M. S. *Phys. Rev. C* **1999**, *60*, 041601.

[3] Boztosun, I.; Rae, W. D. M. *Phys. Rev. C* **2001**, *64*, 054607.

[4] Boztosun, I.; Rae, W. D. M. *Physics Letter B* **2001**, *518*, 229-234.

[5] Boztosun, I. Phys. *Atomic Nuclei* **2002**, *65*, 607-611.

[6] Karakoc M.; Boztosun, I. *Phys. Rev. C* **2006**, *73*, 047601.

[7] Boztosun, I.; Bayrak. O.; Dagdemir, Y. *Int. J. Mod. Phys. E* **2005**, *14*, 663-673.

[8] Boztosun, I.; Dagdemir, Y.; Bayrak. O. *Atomic Nuclei* **2005**, *68*, 1153-1159.

[9] Berry, M. V.; Mount, K. L. *Rep. Prog. Phys.* **1972**, *35*, 315-394.

[10] Brink, D. M.; Takigawa, N. *Nucl. Phys. A* **1977**, *279,* 159-188.

[11] Bayrak, O.; Boztosun, I. *Physics of Atomic Nuclei* **2011**, *74*, 13-18.

[12] Satchler, G. R. *Direct Nuclear Reactions;* Oxford University Press: Oxford, UK, 1983.